AERODYNAMIC ANALYSIS ON MANEUVER CONTROL FOR THE MORPHING WING

Vasile PRISACARIU

”Henri Coandă” Air Force Academy, Braşov, Romania (prisacariu.vasile@afahc.ro)

DOI: 10.19062/1842-9238.2025.23.2.2

Abstract: *The morphing concept has generated emerging technologies in the last decades, from aerodynamic and actuation approaches to advanced materials and artificial intelligence-based control methods that can be used in unmanned aircraft. These approaches can be seen to be focused both on the aerodynamic efficiency and the response speeds of the solutions of the adopted systems. The comparative numerical analyses in the paper consider a series of aspects regarding the translation of the center of pressure and the continuity of the surface, numerical aspects managed by the computational methods of the XFLR5 software tool.*

The article aims to quantify the aerodynamic performance values in the cases of 3D maneuver control of a morphing rectangular wing using the VLM method and the XFLR5 software tool.

Keywords: *morphing wing, aileron, VLM, XFLR5, aerodynamic analysis, NACA 2405*

Acronyms and symbols

c_L ,c_D	*lift and drag coefficient*	c_{mx},c_{my},c_{mz}	*moment coefficients*
c_a, b_a	*Chord and lenght aileron*	δ_A	*Aileron turning angle*
AoA	*Angle of attack*	*BM*	*Bending moment*
CP	*Pressure coefficient*	L_A	*Roll moment*
LLT	*Lifting Line theory*	*S*	*Wing surface*
VLM	*Vortex Lattice Method*	*b*	*Span wing*
V	*Speed*		

1. INTRODUCTION

1.1. General consideration

The morphing concept has generated emerging technologies in recent decades, from aerodynamic and actuation approaches to advanced materials and artificial intelligence-based control methods. These approaches are noted to be focused on both aerodynamic efficiency and response speeds of the adopted system solutions.

According to the literature in the field, aerodynamic analyses regarding maneuver control for biologically inspired morphing wings (variable shape/geometry) are focused on numerical and experimental evaluations regarding the influence of geometry modification on aerodynamic performance and 3D trajectory control capability.

The main objective of the work is to establish the causal link between the 3D deformations of the 3D surface of a rectangular wing and the aerodynamic response (forces and moments) regarding the maneuver control on the 3 axes (roll, pitch, yaw). Objective achieved using the XFLR5 software tool through a series of comparative numerical analyses applied to relatively thin airfoil geometries (NACA 2405 profile).

1.2. Morphing concept

The morphing concept applied to aircraft is treated multidisciplinary in a vast series of authors in recent works, including: *Najmul Mowla et all* in 2025 [1], *Srivastava et all* in 2025 [2], *Majid et all* in 2021 [3], *Pecora et all* in 2021 [4], *Zhu* in 2025 [5], *Chu et all* in 2022 [6], *Dong et all* in 2025 [7], *Budholiya et all* in 2021 [8], *Kabir et all* in 2023 [9] and *Tavarez et all* in 2025 [20].

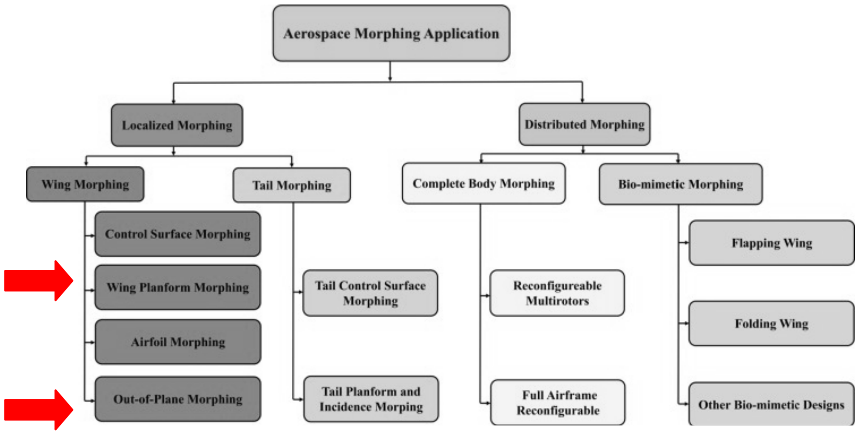

FIG. 1 Morphing classification and application, [1]

A number of recent references outline diverse approaches to evaluating the performance of morphing wings, such as: aerodynamic analyses *Hui et all* in 2020 [10], *Bardera et all* in 2020 [11], *Arai et all* in 2024 [12], *Jini Raj, Bruce* in 2023 [13], *Bardera et all* in 2021 [14], *Abdessemed et all* in 2022 [15], *Negahban et all* in 2024 [16]; experimental analyses *Pan et all* in 2024 [17], *Pecora et all* in 2021 [18], *Zhou et all* in 2022 [19]; use of artificial intelligence *Najmul Mowla et all* in 2025 [1]; actuation methods *Majid et all* in 2021 [3] or aeroelastic *Yuzhu et all* in 2022 [21], *Guo et all* in 2021 [22].

2. THEORETICAL REFERENCES REGARDING AILERON AERODYNAMICS

According to Sadraey 2012 [23], the main function of the ailerons is lateral (roll) control with moment and directional control effects as the ailerons are used symmetrically with different levers, so any change in aileron position/geometry will change the roll rate. The lever deformation of the control surfaces also implies the occurrence of an aerodynamic hinge moment that must be overcome to deform the control surface (the aileron), so a dimensional optimization process is applied to the ailerons to minimize the control forces.

In the process of designing an aileron, a series of parameters are considered (see figure 2), the most relevant being: the aileron area (S_a), the ratio between the chord and the span (length) of the aileron (c_a/b_a), the maximum values of the steering angles (δ_{Amax}) and the aileron position on the span (b_{ai}).

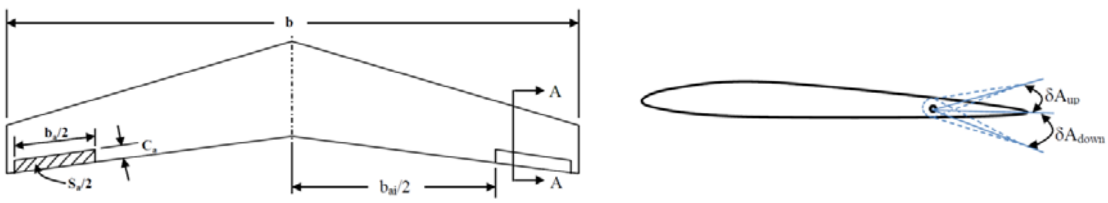

FIG. 2 Aileron geometry, [23]

The maneuverability of an aircraft is a sum of factors considered in the design of the ailerons, such as: the required articulation moment, the effectiveness of the aileron, aerodynamic balancing, the shape (geometry of the ailerons), the type of aircraft structure and the cost of making the ailerons.

As a basic characteristic, the aileron rolling moment (LA) has the equation 1:

$$L_A = 2 \cdot \Delta L \cdot y_A \tag{1}$$

where y_A- the force arm (from the longitudinal axis to the point of application of the force)
ΔL- the variation of the rolling moment

The overall moment on the wing (L_A) is expressed by equation 2:

$$L_A = \frac{1}{2} \cdot \rho \cdot V^2 \cdot S \cdot C_l \cdot b \tag{2}$$

where ρ-air density
V-speed
S- wing surface
C_l- rolling moment coefficient (depending on aircraft configuration)
b- anvewing span

An estimate of the rolling moment (due to lift distribution) for an aileron based on *the strip integration method* has equation 3:

$$\Delta C_l = \frac{C_{LA} \cdot C_a \cdot y_A \cdot dy}{S \cdot b} \tag{3}$$

wheree C_{LA}- the lift coefficient of the section containing the aileron
C_a-aileron chord
y_A- the force arm (from the longitudinal axis to the point of application of the force)
S- wing surface
b- wing span

and the lift coefficient of the section containing the aileron C_{LA} has equation 4:

$$C_{LA} = C_{L\alpha} \cdot \tau_a \cdot \delta_A \tag{4}$$

where $C_{L\alpha}$ – the lift coefficient of the section with the aileron turned
τ_a – aileron effectiveness parameter
δ_A-aileron rotation angle

Figure 3 highlights the dependence of the variation of aileron effectiveness as a function of the ratio between the aileron area (S_a) and the chord of the wing's airfoil (c).

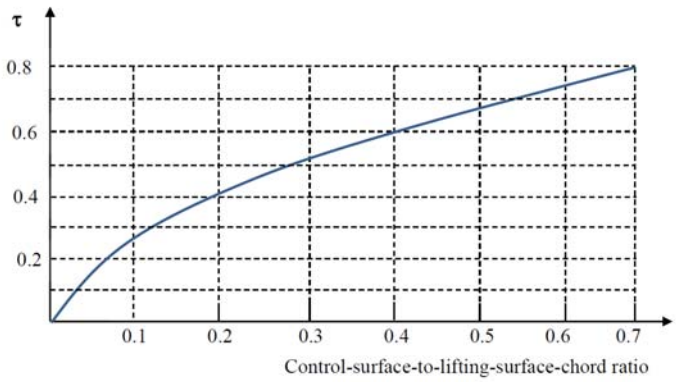

FIG. 3 Aileron efectiveness, [23]

3. LIMITATIONS, METHODS AND SOFTWARE TOOLS

3.1. Limitations of the aerodynamic analyses used

Maneuver control using the morphing concept involves a series of challenges that need to be analyzed, as follows: aerostructural (aeroelastic) coupling regarding aerodynamic deformations coupled with structural deformations, translation of the center of pressure that modifies static stability, 3D surface continuity involving geometric inflections due to the deformation process, response speed that involves dynamic analyses of the actuation systems that determine the 3D deformation of the geometry.

The comparative numerical analyses in the paper consider a series of aspects regarding the translation of the center of pressure and the continuity of the surface, numerical aspects managed by the calculation methods of the XFLR5 software tool. The numerical analyses focus on a series of aerodynamic parameters, such as: the variation of the aerodynamic coefficients of lift Δc_L, and drag Δc_D, the variation of the moment coefficients: pitch Δc_{mx}, roll Δc_{my} and yaw Δc_{mz} and the variation of the aerodynamic smoothness $\Delta c_L/c_D$.

3.2. Vortex Lattice Method

VLM is a numerical method used in fluid mechanics in the pre-design phases of aircraft and in academia. The method models airfoils (wings, empennages) as a thin web of discrete vortices for the calculation of lift and induced drag, the aspects determined by thickness and viscosity being omitted. By simulating the flow field, the pressure and force distribution around the simulated body can be calculated from which the aerodynamic coefficients and their derivatives are extracted for the evaluation of the aircraft's handling qualities in the conceptual design phase.

The VLM method is comprehensively described in a number of aerodynamics works, such as: *Katz & Plotkin* in 2001 [25], *Anderson* in 1991 [26], *Bertin & Smith* in 1998 [27], *Houghton & Carpenter* in 1993 [28], or *Drela* in 2014, [29].

The method is designed on the ideal flow theory (potential flow theory) which neglects the effects of flow viscosity and does not resolve the given aspects of turbulence and boundary layer. It is based on a series of assumptions, the most relevant of which are: the flow field is incompressible, inviscid and irrotational; modeling of compressible subsonic flow with small perturbations with the 3D Prandtl-Glauert transformation; the lifting surfaces are thin, the influence of thickness on aerodynamic forces is neglected; the angle of attack and the glide angle are small.

So the flow field is a conservative vector field, so the local velocity vector (V) is given by equation 5:

$$\boldsymbol{V} = \boldsymbol{V}_\infty + \boldsymbol{\nabla}_{\boldsymbol{\varphi}} \tag{5}$$

where $\boldsymbol{V}_\infty$*- the speed vector of the undisturbed current*

$\boldsymbol{\nabla}_{\boldsymbol{\varphi}}$- *φ satisfies the Laplace equation (2nd order linear equation)*

3.3. XFLR5

It is freeware tool used in the preliminary design phase (based on XFOIL) for 2D and 3D aerodynamic analyses of individual wings and complete aircraft at low Reynolds numbers for gliders, RC models and UAVs. The main modules are:

-2D analysis of wing airfoil through: direct analysis, inverse analysis, aerodynamic airfoil generation and modification, serial analysis;

-3D analysis through geometric modeling of the aircraft, 3D aerodynamic analysis (LLT, VLM, 3D panel method) and aircraft stability analysis;

-visualization and comparison through graphic visualization, flow field visualization.

XFLR5 has a number of limitations, the most relevant being: analyses at low Reynolds numbers and using the incompressible flow assumption (being inaccurate at transonic and supersonic speeds. The XFLR5 instrument user menu includes functions corresponding to the previously described modules, such as: file management commands (new project, open project, insert project save/saveas project), aerodynamic analysis modules (direct/inverse analysis, wing/aircraft design).

4. 3D COMPARATIVE NUMERICAL ANALYSES

4.1. Methodology and analysis conditions

The objective of the numerical analyses is to highlight the influence of using a morphing lateral maneuver concept (twist wing aileron) for a lifting surface versus the constructive solution with classic ailerons.

Table 1. 3D geometry

Features	Value	Features	Value
Span	2 m	Aspect ratio	10
Chord	0,2 m	Taper ratio	1
Lever Aileron angle	± 20 º	Mesh elements	494 / 416 / 494
Airfoil	NACA 2405		

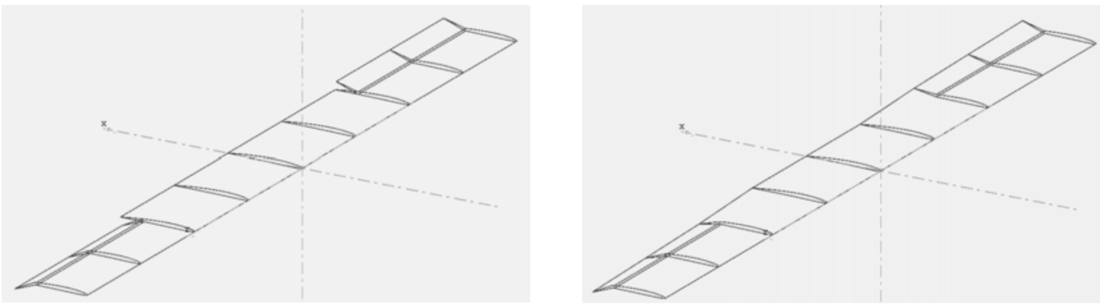

a b

FIG. 4 Wing geometry for analysis, a. with classic ailerons, b. with morphing ailerons

The analysis objectives are instrumented with XFLR 6.61 applied to a 3D wing geometry in three variants: plank wing, classic ailerons wing and morphing ailerons wing (see table 1 and FIG. 4). The numerical analysis conditions and simulation cases are based on the Vortex Lattice Method (VLM) described in the previous chapter and are indicated in Table 2.

Table 2. Analysis conditions

Condition	Value	Condition	Value
Nr. iteration	100	Analysis method	VLM1
Polar type	Fixed speed	Vortex position VLM	25%
Alpha precision	0,01	Control point position VLM	75%
Speed	10 m/s	AoA	$-15^o \div 15^o$
Air density	1,225 kg/m^3	Air viscosity	1,5 x 10^{-5} m^2/s

4.2.Results and discussions

The comparative results of the numerical simulations for the 3 geometries are presented in the figures below. All comparative polars indicate the influence of the geometry change on the analyzed angle of attack range.

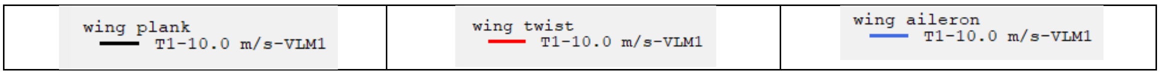

Figure 5a indicates a minimal influence of geometry on the lift coefficient. Figure 5b as expected shows an increase in the drag coefficient C_D for the hinged wing variants.

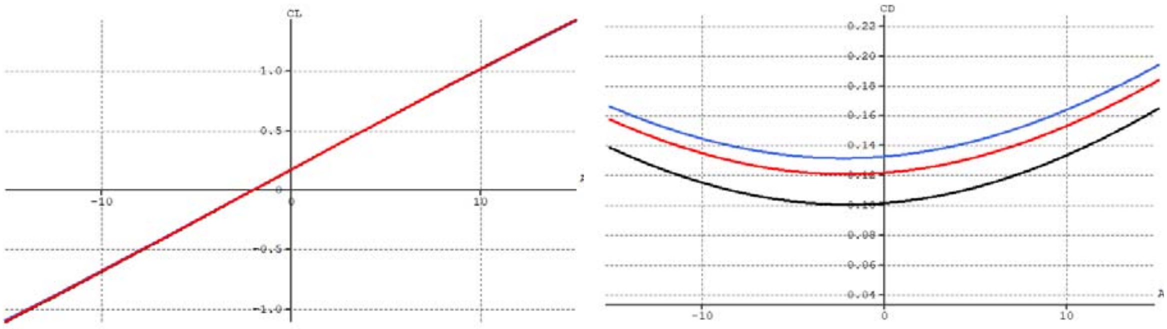

a b

FIG. 5 Polars C_L și C_D, a. C_L vs AoA, b. C_D vs AoA

The graph in figure 6a indicates a minimal influence of the geometries with turns on the pitching moment coefficient C_m , while the roll coefficient C_l is higher in the case of classic ailerons (0.17), also noting the efficiency of morphing ailerons at zero angle of attack (0.14).

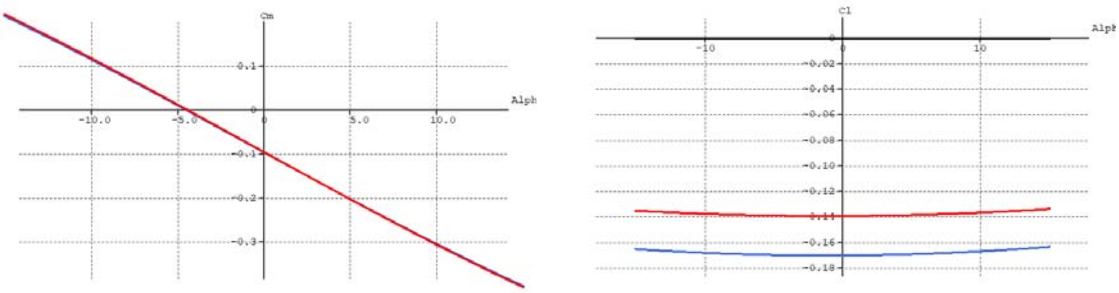

a b

FIG. 6 Polars C_m și C_l, a. C_m vs AoA, b. C_l vs AoA

Figure 7a indicates a similar behavior for the roll motion through values of the roll coefficient C_n , and figure 7b shows higher values of the hinge moment (BM) in the case of classical ailerons (over the range AoA =-3°÷3°).

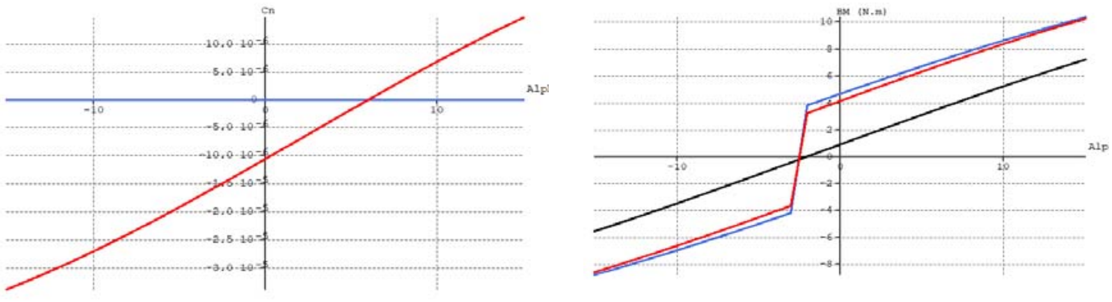

a b

FIG. 7 C_n polar and BM chart, a. C_n vs AoA, b. BM vs AoA

Figure 8 shows the distribution of airfoils for the wing at AoA=0o in the two geometric configurations, we note the reduction of turbulence in the geometric inflection areas of the morphing ailerons (fig. 8b).

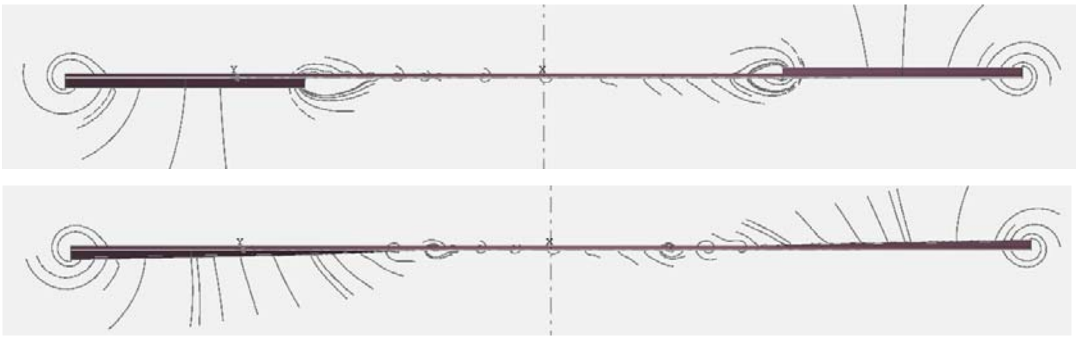

a

b

FIG. 8 Airflow distribution wing, a. classic aileron wing, b. morphing aileron wing

As an additional argument for modifying the drag coefficient (CD) for the two geometries (FIG. 5b) we have differences regarding the induced drag profile for angle of attack AoA= 0o (see FIG. 9).

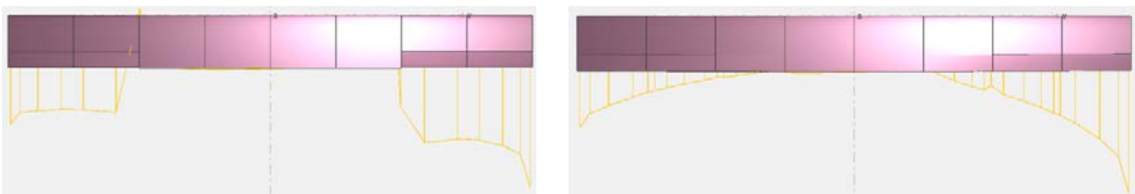

a b

FIG. 9 Induced drag, a. classic aileron wing, b. morphing aileron wing

The influence on the pressure coefficient (CP) coordinates due to the change in geometry given by the rotations of the classic ailerons vs. morphing is found in the data in table 3, for values at AoA= 0^{o}, where we have a smaller lateral displacement of the CP for the morphing wing versus the classic aileron wing.

Table 3. CP coordinate

3D geometry	**X_{cp} mm**	**Y_{cp} mm**	**Z_{cp} mm**
Wing plank	112,741	0	3,402
Wing classic aileron	112,064	1986,979	-1,693
Wing morphing aileron	112,185	1641,757	0,146

After the analyses, a lower maneuvering efficiency is observed in the case of the geometry with morphing ailerons, considering the similar extreme rotate angles (±20°). Therefore, a higher steering value of the morphing ailerons or the use of a larger useful area is required, an aspect that is also found in the series of equations exposed in the theoretical chapter. For an evaluation of the aerodynamic qualities of the selected 2D (NACA 2405) and 3D wing geometries, we can also consult the appendix with the numerical simulation values.

CONCLUSION

The paper presented a software analysis case regarding the influence of geometric modifications of the classic/morphing aileron type on the maneuverability of aircraft, a case based on software simulations on a 3D single wing geometry.

The morphing concept used in 3D maneuver cases involves increasing the active area and/or the rotation angle to obtain similar values of the rolling moment as in the case of classic (articulated) ailerons. An advantage of morphing ailerons is the reduction of drag and a minimization of turbulence due to the geometric inflection zones of the ailerons in the near of the unsteering surfaces (see figure 8).

The paperwork can be considered a first step in the study of performance analyses applied to fixed airfoils in the construction of unmanned aircraft with classic or morphing concept maneuvering/control surfaces.

Future analyses can be based on morphing geometries with a higher degree of fidelity and to quantify the effects of using morphing geometries in maneuvering cases, the use of finite element CFD numerical simulations is required for a more accurate visualization of the values of the moment coefficients due to geometric changes.

REFERENCES

[1] Md. N. Mowla, D. Asadi, T. Durhasan, J. R. Jafari, M. Amoozgar, Recent advancements in morphing applications: Architecture, artificial intelligence integration, challenges, and future trends-a comprehensive survey, Aerospace Science and Technology, Volume 161, 2025, 110102,ISSN 1270-9638, https://doi.org/10.1016/j.ast.2025.110102;

[2] Srivastava, Sudhanshu & Patel, Nayankumar & Padhiyar, Mehul & Bhardwaj, Ravi. Morphing Aircraft Wing: Development and Application. International Journal of All Research Education and Scientific Methods. 13. 1294-1302. 10.56025/IJARESM.2025.1305251294, 2025;

[3] Majid, Tuba & Jo, Bruce, *Status and Challenges on Design and Implementation of Camber Morphing Mechanisms*, International Journal of Aerospace Engineering. 1-14. 10.1155/2021/6399937, 2021;

[4] R. Pecora, *Morphing wing flaps for large civil aircraft: evolu-tion of a smart technology across the Clean Sky program*, Chinese Journal of Aeronautics, vol. 34, no. 7, pp. 13–28, 2021 (PDF) Status and Challenges on Design and Implementation of Camber Morphing Mechanisms;

[5] H. Zhu, *History and Future Development of Morphing-Wing Aircrafts,* Theoretical and Natural Science, 86,120-125 , 2025;

[6] L.L. Chu, Q. Li, F. Gu, X.T. Du, Y.Q. He, Y.C. Deng, *Design, modeling, and control of morphing aircraft: A review*, Chinese Journal of Aeronautics, 35 (5), 220-246, 2022;

[7] Chengyue Dong, Mansur M. Arief, Morphing Wing Designs in Commercial Aviation, 11 Feb 2025, arXiv:2502.07182v1 , available at https://arxiv.org/html/2502.07182v1;

[8] S. Budholiya, A. Bhat, S.A. Raj et al, *State of the art review about bio-inspired design and applications: an aerospace perspective*, Appl Sci 2021; 11(11): 5054;

[9] A. Kabir, A.S.M. Al-Obaidi,F.W.Y. Myan, Review and aerodynamic analysis of NACA 2415 morphing wing for variable span and scale morphing concepts using CFD analysis, Journal of Physics: Conference Series, 1/2023, vol 2523, ISSN 1742-6596, doi 10.1088/1742-6596/2523/1/012033, https://doi.org/10.1088/1742-6596/2523/1/012033;

[10] Z. Hui, Y. Zhang, G. Chen, Tip-vortex flow characteristics investigation of a novel bird-like morphing discrete wing structure. Phys Fluids 2020; 32(3): 035112;

[11] R. Bardera, A. Garcia-Magariño, E.B. Barderas et al., *Analysis of the tip vortex in the wake of a bioinspired morphing MAV*, In: AIAA AVIATION 2020 FORUM. Reston, Virginia: American Institute of Aeronautics and Astronautics, 2020;

[12] Y. Arai, H. Tanaka, & M. Kashitani, *Evaluation of aerodynamic characteristics of a twist morphing wing consisting of lattice structure*, In Asia Pacific International Symposium On Aerospace Technology (APISAT 2024). Engineers Australia, available at https://search.informit.org/doi/10.3316 /informit.T2025031300020492055755843, 2024;

[13] R. Jini Raj, R.R.J. Bruce, *Flow physics and boundary layer optimization over a NACA airfoil by camber morphing at subsonic speeds*, Int J Mod Phys C 2023; 34(6): 2350080;

[14] R. Bardera, Á.A. Rodríguez-Sevillano, E. Barroso, *Numerical and experimental study of aerodynamic performances of a morphing Micro Air Vehicle*, Applied Mechanics 2021; 2(3): 442–459;

[15] C. Abdessemed, A. Bouferrouk, Y. Yao, Effects of an unsteady morphing wing with seamless side-edge transition on aerodynamic performance. Energies 2022; 15(3): 1093;

[16] M.H. Negahban, M. Bashir, V. Traisnel, R.M. Botez, *Seamless morphing trailing edge flaps for UAS-S45 using high-fidelity aerodynamic optimization*, Chinese Journal of Aeronautics, Volume 37, Issue 2, 2024, Pages 12-29, ISSN 1000-9361;

[17] G. Pan, X. Cui, P. Sun, B. Wang, *A Brief Review of the Actuation Systems of the Morphing Systems in Wind Tunnel Models and a Case Study*, Aerospace 2024, 11, 666, https://doi.org/10.3390/ aerospace11080666;

[18] R. Pecora, F. Amoroso, M.S. Sicim, *Design of a Morphing Test-Article for Large-Scale, High-Speed Wind Tunnel Tests of an Adaptive Wing Flap*, In Active and Passive Smart Structures and Integrated Systems XV; SPIE: Bellingham, WA, USA, 2021; Volume 11588;

[19] H. Zhou, A. R. Plummer and D. Cleaver, *Distributed Actuation and Control of a Tensegrity-Based Morphing Wing*, in IEEE/ASME Transactions on Mechatronics, vol. 27, no. 1, pp. 34-45, Feb. 2022, doi: 10.1109/TMECH.2021.3058074. keywords;

[20] S.M.O. Tavares, P.V. Gamboa, P.M.S.T. de Castro, *Aircraft Wings and Morphing–Evolution of the Concepts,* Encyclopedia 2025, 5, 101, available at https://doi.org/10.3390/encyclopedia5030101;

[21] L. Yuzhu, G. Wenjie, Z. Jin, Y. Zhang, Z. Donglai, W. Zhuo, D. Dianbiao, Design and experiment of concentrated flexibility-based variable camber morphing wing. Chinese Journal of Aeronautics 2022; 35(5):455-69;

[22] Q. Guo, X. He, Z. Wang, et al, *Effects of wing flexibility on aerodynamic performance of an aircraft model*, Chin J Aeronaut 2021; 34(9): 133–142;

[23] M. Sadraey, *Aircraft design: A System Engineering Approach*, 2012, ISBN:9781119953401 792p. John Wiley & Sons, Ltd;

[24] D. Li, Y. Wu, A. Da Ronch, J. Xiang, *Energy harvesting by means of flow-induced vibrations on aerospace vehicles*, Progress in Aerospace Sciences, Volume 86, 2016, Pages 28-62, ISSN 0376-0421;

[25] J. Katz, A. Plotkin, *Low-Speed Aerodynamics*, 2001, Cambridge Aerospace Series, 630p, ISBN 978-0521665520;

[26] J.D. Anderson Jr, *Fundamentals of aerodynamics*, 2nd ed., McGraw-Hill Inc, 1991, 792p. . ISBN, 978-0071007672;

[27] J.J. Bertin, M.L. Smith, *Aerodynamics for Engineers*, 3rd ed., Prentice Hall, New Jersey, 1998. ISBN 978-0631190738;

[28] E.L. Houghton, P.W. Carpenter, *Aerodynamics for Engineering Students*, 4th ed., Edward Arnold, London, 1993, ISBN 978-0340548479;

[29] M. Drela, *Flight Vehicle Aerodynamics, MIT Press*, Cambridge, MA, 2014. ISBN 978-0262526449;

[30] M. Drela, Analysis of foils and wings operating at low Reynolds numbers, *Guidelines for XFLR5 v6.03, 2011, 71p*.

APPENDIX

Wing twist

Plane name : wing twist
Polar name : T1-10.0 m/s-VLM1
Freestream speed : 10.000 m/s

alpha	Beta	CL	CDi	CDv	CD	CY	Cl	Cm	Cn	Cni	QInf	XCP
-15.000	0.000	-1.098358	0.057091	0.100091	0.157182	0.000271	-0.135088	0.216685	-0.000034	-0.000034	10.0000	0.0403
-14.000	0.000	-1.016580	0.051857	0.100091	0.151948	0.000263	-0.135654	0.197431	-0.000033	-0.000033	10.0000	0.0394
-13.000	0.000	-0.934220	0.046977	0.100091	0.147068	0.000255	-0.136179	0.177852	-0.000031	-0.000032	10.0000	0.0384
-12.000	0.000	-0.851300	0.042465	0.100091	0.142557	0.000246	-0.136662	0.157971	-0.000030	-0.000030	10.0000	0.0372
-11.000	0.000	-0.767872	0.038338	0.100091	0.138430	0.000238	-0.137104	0.137817	-0.000029	-0.000029	10.0000	0.0358
-10.000	0.000	-0.683984	0.034609	0.100091	0.134700	0.000229	-0.137504	0.117409	-0.000027	-0.000027	10.0000	0.0340
-9.000	0.000	-0.599682	0.031290	0.100091	0.131381	0.000220	-0.137861	0.096770	-0.000026	-0.000026	10.0000	0.0318
-8.000	0.000	-0.515015	0.028393	0.100091	0.128484	0.000210	-0.138177	0.075929	-0.000024	-0.000024	10.0000	0.0288
-7.000	0.000	-0.430031	0.025927	0.100091	0.126018	0.000201	-0.138451	0.054909	-0.000022	-0.000023	10.0000	0.0247
-6.000	0.000	-0.344780	0.023901	0.100091	0.123992	0.000191	-0.138682	0.033736	-0.000021	-0.000021	10.0000	0.0185
-5.000	0.000	-0.259311	0.022321	0.100091	0.122413	0.000182	-0.138871	0.012434	-0.000019	-0.000020	10.0000	0.0082
-4.000	0.000	-0.173674	0.021195	0.100091	0.121286	0.000172	-0.139018	-0.008970	-0.000018	-0.000018	10.0000	-0.0125
-3.000	0.000	-0.087919	0.020526	0.100091	0.120617	0.000162	-0.139122	-0.030451	-0.000016	-0.000016	10.0000	-0.0720
-2.000	0.000	-0.002097	0.020316	0.100091	0.120408	0.000152	-0.139184	-0.051982	-0.000014	-0.000014	10.0000	-5.0198
-1.000	0.000	0.083742	0.020569	0.100091	0.120660	0.000141	-0.139204	-0.073539	-0.000012	-0.000013	10.0000	0.1767
0.000	0.000	0.169547	0.021283	0.100091	0.121374	0.000131	-0.139181	-0.095096	-0.000011	-0.000011	10.0000	0.1122
1.000	0.000	0.255268	0.022458	0.100091	0.122549	0.000121	-0.139115	-0.116626	-0.000009	-0.000009	10.0000	0.0918
2.000	0.000	0.340853	0.024090	0.100091	0.124181	0.000110	-0.139007	-0.138103	-0.000007	-0.000007	10.0000	0.0805
3.000	0.000	0.426253	0.026176	0.100091	0.126267	0.000100	-0.138857	-0.159502	-0.000005	-0.000006	10.0000	0.0743
4.000	0.000	0.511417	0.028710	0.100091	0.128801	0.000089	-0.138664	-0.180798	-0.000004	-0.000004	10.0000	0.0701
5.000	0.000	0.596297	0.031685	0.100091	0.131776	0.000079	-0.138429	-0.201964	-0.000002	-0.000002	10.0000	0.0671
6.000	0.000	0.680842	0.035093	0.100091	0.135184	0.000068	-0.138152	-0.222976	-0.000000	-0.000000	10.0000	0.0649
7.000	0.000	0.765004	0.038925	0.100091	0.139016	0.000058	-0.137832	-0.243807	0.000002	0.000001	10.0000	0.0632
8.000	0.000	0.848735	0.043168	0.100091	0.143259	0.000047	-0.137471	-0.264433	0.000003	0.000003	10.0000	0.0619
9.000	0.000	0.931987	0.047812	0.100091	0.147903	0.000037	-0.137068	-0.284830	0.000005	0.000005	10.0000	0.0608
10.000	0.000	1.014714	0.052842	0.100091	0.152933	0.000027	-0.136622	-0.304973	0.000007	0.000006	10.0000	0.0599
11.000	0.000	1.096870	0.058244	0.100091	0.158335	0.000016	-0.136136	-0.324837	0.000008	0.000008	10.0000	0.0591
12.000	0.000	1.178410	0.064001	0.100091	0.164093	0.000006	-0.135607	-0.344400	0.000010	0.000010	10.0000	0.0585
13.000	0.000	1.259290	0.070098	0.100091	0.170189	-0.000004	-0.135037	-0.363636	0.000012	0.000011	10.0000	0.0579
14.000	0.000	1.339467	0.076516	0.100091	0.176607	-0.000014	-0.134426	-0.382525	0.000013	0.000013	10.0000	0.0575
15.000	0.000	1.418899	0.083235	0.100091	0.183326	-0.000024	-0.133775	-0.401042	0.000015	0.000014	10.0000	0.0571

Wing aileron

Plane name : wing aileron
Polar name : T1-10.0 m/s-VLM2
Freestream speed : 10.000 m/s

alpha	Beta	CL	CDi	CDv	CD	CY	Cl	Cm	Cn	Cni	QInf	XCP
-15.000	0.000	-1.089544	0.065790	0.100098	0.165888	-0.000000	-0.165105	0.212632	-0.000000	-0.000000	10.0000	0.0399
-14.000	0.000	-1.008196	0.060775	0.100098	0.160873	-0.000000	-0.165791	0.193554	-0.000000	-0.000000	10.0000	0.0390
-13.000	0.000	-0.926262	0.056104	0.100098	0.156203	-0.000000	-0.166427	0.174177	-0.000000	0.000000	10.0000	0.0380
-12.000	0.000	-0.843784	0.051794	0.100098	0.151892	-0.000000	-0.167013	0.154502	-0.000000	0.000000	10.0000	0.0368
-11.000	0.000	-0.760818	0.047858	0.100098	0.147957	-0.000000	-0.167547	0.134555	-0.000000	0.000000	10.0000	0.0353
-10.000	0.000	-0.677383	0.044311	0.100098	0.144409	-0.000000	-0.168031	0.114358	-0.000000	-0.000000	10.0000	0.0335
-9.000	0.000	-0.593552	0.041163	0.100098	0.141262	-0.000000	-0.168463	0.093936	-0.000000	-0.000000	10.0000	0.0312
-8.000	0.000	-0.509364	0.038426	0.100098	0.138525	-0.000000	-0.168844	0.073313	-0.000000	-0.000000	10.0000	0.0282
-7.000	0.000	-0.424867	0.036110	0.100098	0.136208	-0.000000	-0.169174	0.052514	-0.000000	0.000000	10.0000	0.0239
-6.000	0.000	-0.340109	0.034221	0.100098	0.134320	-0.000000	-0.169452	0.031564	-0.000000	0.000000	10.0000	0.0175
-5.000	0.000	-0.255139	0.032768	0.100098	0.132867	-0.000000	-0.169678	0.010489	-0.000000	-0.000000	10.0000	0.0070
-4.000	0.000	-0.170007	0.031756	0.100098	0.131854	-0.000000	-0.169853	-0.010687	-0.000000	-0.000000	10.0000	-0.0142
-3.000	0.000	-0.084762	0.031188	0.100098	0.131287	-0.000000	-0.169976	-0.031938	-0.000000	0.000000	10.0000	-0.0780
-2.000	0.000	0.000545	0.031068	0.100098	0.131167	0.000000	-0.170047	-0.053239	-0.000000	-0.000000	10.0000	15.8309
-1.000	0.000	0.085865	0.031397	0.100098	0.131496	0.000000	-0.170066	-0.074564	-0.000000	-0.000000	10.0000	0.1746
0.000	0.000	0.171148	0.032175	0.100098	0.132274	0.000000	-0.170034	-0.095887	-0.000000	-0.000000	10.0000	0.1121
1.000	0.000	0.256344	0.033401	0.100098	0.133499	0.000000	-0.169950	-0.117183	-0.000000	0.000000	10.0000	0.0911
2.000	0.000	0.341403	0.035070	0.100098	0.135169	0.000000	-0.169814	-0.138427	-0.000000	0.000000	10.0000	0.0806
3.000	0.000	0.426276	0.037181	0.100098	0.137279	0.000000	-0.169626	-0.159592	-0.000000	-0.000000	10.0000	0.0743
4.000	0.000	0.510911	0.039726	0.100098	0.139824	0.000000	-0.169387	-0.180654	-0.000000	-0.000000	10.0000	0.0702
5.000	0.000	0.595264	0.042699	0.100098	0.142797	0.000000	-0.169096	-0.201587	-0.000000	-0.000000	10.0000	0.0672
6.000	0.000	0.679283	0.046091	0.100098	0.146190	0.000000	-0.168754	-0.222366	-0.000000	-0.000000	10.0000	0.0645
7.000	0.000	0.762919	0.049894	0.100098	0.149992	0.000000	-0.168360	-0.242967	-0.000000	-0.000000	10.0000	0.0632
8.000	0.000	0.846127	0.054096	0.100098	0.154194	0.000000	-0.167915	-0.263164	-0.000000	-0.000000	10.0000	0.0619
9.000	0.000	0.928860	0.058685	0.100098	0.158783	0.000000	-0.167418	-0.283533	-0.000000	0.000000	10.0000	0.0607
10.000	0.000	1.011070	0.063647	0.100098	0.163745	0.000000	-0.166871	-0.303449	-0.000000	0.000000	10.0000	0.0598
11.000	0.000	1.092718	0.068968	0.100098	0.169067	0.000000	-0.166273	-0.323090	-0.000000	-0.000000	10.0000	0.0591
12.000	0.000	1.173746	0.074633	0.100098	0.174732	0.000000	-0.165624	-0.342431	-0.000000	-0.000000	10.0000	0.0584
13.000	0.000	1.254124	0.080625	0.100098	0.180723	0.000000	-0.164925	-0.361450	-0.000000	0.000000	10.0000	0.0579
14.000	0.000	1.333805	0.086925	0.100098	0.187024	0.000000	-0.164175	-0.380123	-0.000000	0.000000	10.0000	0.0574
15.000	0.000	1.412748	0.093515	0.100098	0.193614	0.000000	-0.163376	-0.398427	-0.000000	-0.000000	10.0000	0.0570